PLoS ONE

Nanostructured Oxygen Sensor - Using Micelles to Incorporate a Hydrophobic Platinum Porphyrin

Fengyu Su, Ruhaniyah Alam, Qian Mei, Yanqing Tian*, Cody Youngbull, Roger H. Johnson, Deirdre R. Meldrum

Center for Biosignatures Discovery Automation, Biodesign Institute, Arizona State University, Tempe, Arizona, United States of America

Abstract

Hydrophobic platinum(II)-5,10,15,20-tetrakis-(2,3,4,5,6-pentafluorophenyl)-porphyrin (PtTFPP) was physically incorporated into micelles formed from poly(ε-caprolactone)-*block*-poly(ethylene glycol) to enable the application of PtTFPP in aqueous solution. Micelles were characterized using dynamic light scattering (DLS) and atomic force microscopy (AFM) to show an average diameter of about 140 nm. PtTFPP showed higher quantum efficiency in micellar solution than in tetrahydrofuran (THF) and dichloromethane (CH_2Cl_2). PtTFPP in micelles also exhibited higher photostability than that of PtTFPP suspended in water. PtTFPP in micelles exhibited good oxygen sensitivity and response time. This study provided an efficient approach to enable the application of hydrophobic oxygen sensors in a biological environment.

Introduction

Dissolved oxygen concentrations in live cells and cellular environments are critical for many physiological and pathological processes including metabolism, cell respiration/oxygen consumption, and tissue hypoxia [1–10]. Fluorescence based optical oxygen sensors, such as platinum (II) porphyrins, palladium (II) porphyrins, and ruthenium polypyridyl complexes [11–23] were developed for measuring oxygen concentrations at cellular levels because these optical sensors: (i) are noninvasive; (ii) can be used in not only large, but also in small volumes down to a few picoliters at the single cell level; and (iii) can be integrated with other optical sensors for simultaneously monitoring multi-parameters. These characteristics endow many advantages of the optical approach for oxygen concentration measurement, with which the popularly applied electrochemistry based oxygen sensing method can hardly compete [24]. Some optical oxygen sensing materials and membranes were successfully developed to extracellularly monitor oxygen consumption not only at the microscale, but also with high throughput, as has been demonstrated using bacteria, isolated mitochondria, cellular lines and small organisms [2,5,6,8,9,10]. We have developed new oxygen sensors for extracellular oxygen sensing [25,26,27] and applied these sensors for detecting single cell oxygen consumption [7,8]. Although many oxygen sensors have been reported, there are only a few materials that can be used for intracellular oxygen sensing, as this requires that the sensors be soluble or able to disperse well in water, exhibit good oxygen responses, and have excellent photostability. Water soluble ruthenium tris(diphenyl phenanthroline) (RuDPP) [28] and ruthenium tris(2,2′-dipyridyl)dichloride hexahydrate (RTDP) [29] were used to study intracellular oxygen concentrations. Polymer nanoparticles incorporated with oxygen sensitive fluorophores,

such as the RuDPP and platinum (II) octaethyl porphyrin ketone (PtOEP), were prepared and loaded into cells through microinjection or microprojectile delivery [13,30]. Liposome was utilized to deliver the RuDPP dispersed in polystyrene beads into macrophages through phagocytosis [31]. Hydrophilic metal porphyrins (PtCPK, PtCP, PdCPK, PtTCPP) [32,33,34] were recently studied as molecular intracellular oxygen sensors. However, extremely low quantum efficiencies, in the range of 0.001 to 0.0095, were observed for these hydrophilic metalporphyrin-derived oxygen sensors.

Among the many oxygen sensors, platinum(II)-5,10,15,20-tetrakis-(2,3,4,5,6-pentafluorophenyl)-porphyrin (PtTFPP) is known to be an excellent one due to its good responses to oxygen concentrations, high photostability, and high quantum efficiency as compared with others [35,36]. Unfortunately, its extreme hydrophobicity limits its application in a biological environment. Recently, Borisov et al. reported an incorporation of PtTFPP in polystyrene-*block*-polyvinylpyrrolidone beads and studied the oxygen responses in aqueous solutions [37]. The authors demonstrated that the beads with an average diameter of approximately 250 nm were cell impermeable for *E. coli*. Previously, we used micelles formed from amphiphilic block copolymers to incorporate hydrophobic two-photon absorbing materials and photodynamic therapeutic drugs – porphyrins to deliver the hydrophobic materials into cells [38,39,40]. Along this line, herein, we report the incorporation of PtTFPP in micelles formed from poly(ethylene glycol)-*block*-poly(ε-caprolactone) (PEG-*b*-PCL) (Figure 1) and the evaluation of oxygen responses of PtTFPP-encapsulated micelles. We demonstrated that PtTFPP in micelles showed good oxygen responses and photo-stability in aqueous media. This study may provide an alternative avenue for intracellular oxygen sensor design and investigation.
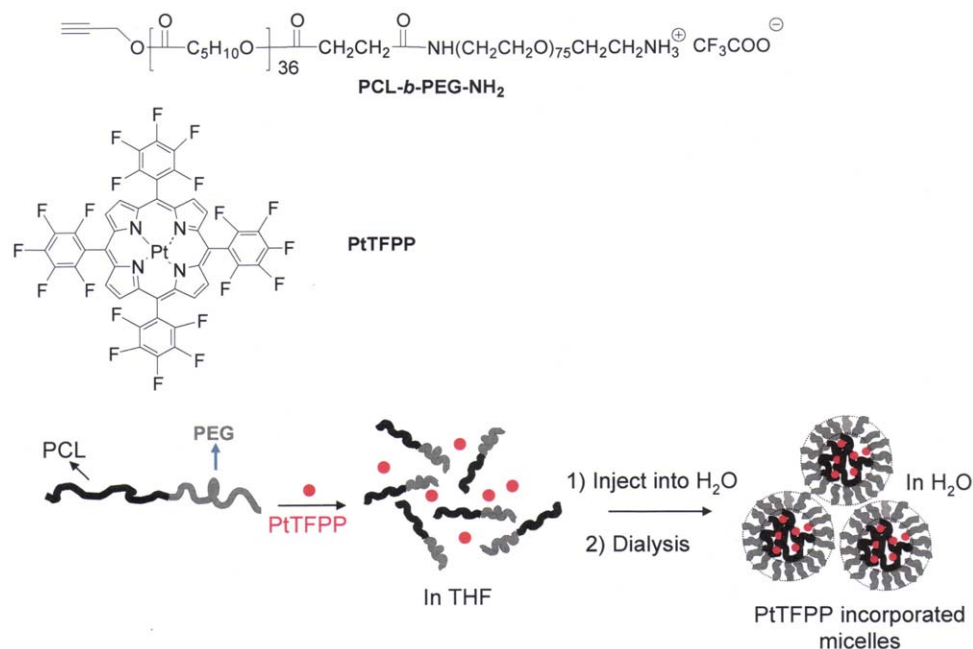
Figure 1. Chemical structures of PtTFPP and PCL-*b*-PEG and the schematic drawing of the micelle formation.
doi:10.1371/journal.pone.0033390.g001

Experiment

Materials

PtTFPP was purchased from Frontier Scientific (Logan Utah), PEG-*b*-PCL [M_n (GPC) = 13300, M_w/M_n = 1.29; M_n (NMR) = 8300] was synthesized according to a previous publication [38]. 4-(2-Hydroxyethyl)-1-piperazineethanesulfonic acid (HEPES) was ordered from Sigma-Aldrich (St. Louis, MO).

Instruments

UV-Vis spectra were recorded with a Shimadzu UV-3600 UV-VIS-NIR spectrophotometer (Shimadzu Scientific Instruments, Columbia, MD). Fluorescence spectra were recorded with a Shimadzu RF-5301 spectrofluorophotometer. Dynamic light scattering (DLS) measurements for micelle diameters were performed using a Malvern Nano-ZS instrument equipped with a 4 mW He-Ne laser (633 nm) with an output at a scattering angle of 173°. The solution was passed through a 0.45 µm Nylon micro-filter (VWR, Batavia, IL) to remove dust before the DLS measurements. Atomic force microscopy (AFM, NanoScope III, Veeco, Plainview, NY) equipped with an integrated silicon tip/cantilever with resonance frequency of ∼240 kHz in height and phase image models was utilized for the observation of morphologies. Polymer solutions (4 µL) were dropped on a mica sample stage and dried at room temperature for morphological observation. The AFM topographies showed no evidence of tip-induced modification during successive scans.

Preparation of micelles

Block copolymer PEG-*b*-PCL (5 mg) and 200 µL of 1 mM PtTFPP in THF were mixed to make a clear solution. The THF solution was added slowly into 1.0 mL of a MilliQ distilled water solution under vigorous stirring. The micelles were transferred to a dialysis bag and dialyzed against MilliQ water for 3 days with a water change of about every 12 hours. The solution was then filtered through a 0.45 µm micro-filter to eliminate excess non-incorporated PtTFPP. The content of PtTFPP in micelles was determined from a standard curve for PtTFPP in THF using an absorbance spectrometer. It was determined that the micelle contained 100 µM of PtTFPP, and the polymer concentration for the micelle stock solution was 2.5 mg/mL. The micelles remained stable in a 4°C refrigerator for at least one month without an alternation of photophysical properties and/or sizes.

Determination of quantum yields

The fluorescence quantum yields (η) of samples in solutions were recorded by using PtTFPP in methylene chloride ($\eta = 0.088$) [41] excited at 390 nm and were calculated according to the following equation [42]:

$$\eta_s = \eta_r \left(\frac{A_r}{A_s} \right) \left(\frac{I_s}{I_r} \right) \left(\frac{n_s^2}{n_r^2} \right) \quad (1)$$

where η_r and η_s are the fluorescence quantum yields of standards and the samples, respectively. A_r and A_s are the absorbance of the standards and the measured samples at the excitation wavelength, respectively. I_r and I_s are the integrated emission intensities of the standards and the samples, respectively. n_r and n_s are the refractive indices of the corresponding solvents of the solutions, respectively.

Oxygen sensing performance

Nitrogen and oxygen gas mixtures were used to saturate the solution to adjust the dissolved oxygen concentrations. The gas mixtures were precisely controlled with a custom-built, in-line, digital gas flow controller. All sensing measurements were carried out at atmospheric pressure, 760 mmHg or 101.3 kPa. At the air saturated condition with an oxygen partial pressure of 21.4 kPa, the dissolved oxygen concentration in water is 8.58 mg/mL at 23°C.

Response time

Response time measured through the bubbling with a mixture of nitrogen and oxygen gas. 3 mL of PtTFPP

micelles was placed in a quartz cuvette. Emission measurements were taken every 4 second at the sensor's peak emission of 650 nm and excited at 405 nm. To vary the concentrations of dissolved oxygen in the buffers, we used a gas manifold to control gas flow through a tube and needle to bubble the buffers. Holes were installed in the cuvette cap to allow the needle into the cuvette and gas flow out. Oxygen and nitrogen flow rates were set at 66 standard cubic centimeters per minute. In all trials, the buffer was first saturated with 21% of oxygen and 79% of nitrogen (to mimic atmospheric condition) before beginning the measurements. Measurements began with an immediate change from the mimic air flow into the buffer to 100% nitrogen, and then continued as the gas flow composition was then immediately reversed between air and nitrogen.

Response time measured using glucose oxidase. 3 mL of PtTFPP micelles was placed in a quartz cuvette. Glucose was added to reach a glucose concentration of 0.25 M. 60 µL of glucose oxidase (concentration: 10 mg/mL) was added into the micelle-glucose solutions. Emission measurements were taken every 0.1 seconds at the sensor's peak emission of 650 nm and excited with 405 nm.

Photostability investigation

The micelle solution (5 µM of PtTFPP) in pH 7.0 B-R buffer was continuously exposed to the excitation light at 405 nm (0.2 mW/cm^2) over a period of 50 minutes. The fluorescence intensity was recorded over an interval of 2 min.

Results and Discussion

Micelle preparation and characterization

Using a dialysis approach as described in the experimental part, PtTFPP was successfully incorporated into the micelles. The block copolymer used for this study is a cationic amino group containing PEG-*b*-PCL (Figure 1). The use of cationic amine-containing groups can enhance the endocytosis ability, which was investigated by other research groups [43,44] as well as by us [38].

Critical micelle concentration (CMC) of this PEG-*b*-PCL copolymer was determined to be 0.37 µM (3.39×10^{-3} mg/mL) [38]. Stability of the micelles formed from PEG-*b*-PCL was investigated previously, showing the micelles were stable in HEPES buffer even with 1000 fold dilution. The micelles were less stable in cell culture medium than in HEPES solution, but can still be stable in cell culture medium with 50 folds dilution [38] most likely because the medium has additional supplements such as sugars, salts, and phenol red. Micelles were characterized using DLS with an average diameter of 140 nm in the aqueous solution (Figure 2A). The micelles were dried at room temperature on mica and although the micelles easily formed a continuous phase, some micelles with an average diameter of 128±12 nm were clearly observed (Figure 2B), which is generally in accordance with the size measured in aqueous solutions.

The micelles were quite stable when stored at 4°C. After one month storage, no size or photophysical property change was observed. Release of PtTFPP from micelles was investigated through the typical release study at 37°C in the HEPES buffer. After a 48 hours release investigation, less than 8% of PtTFPP was released from the micelles or, in other words, more than 92% of PtTFPP was retained in micelles, showing good stability of the PtTFPP incorporated PCL-*b*-PEG micelles (Figure 3).

Photophysical properties

Figure 4 shows the absorption and emission spectra of PtTFPP in micelles compared with those in THF and CH$_2$Cl$_2$ at a PtTFPP
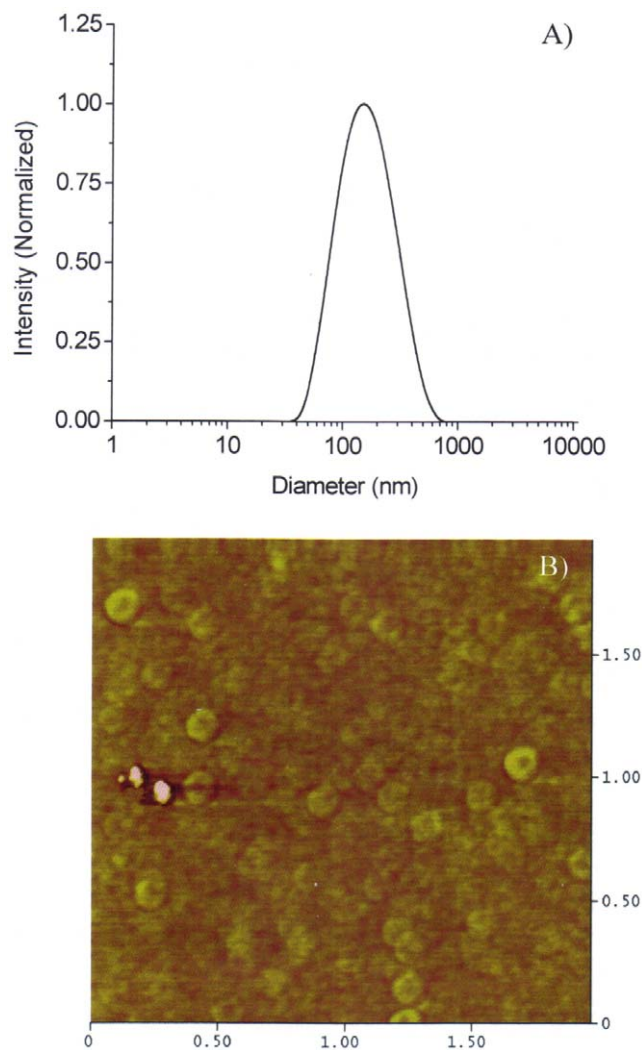

Figure 2. DLS of the micelles (A) and AFM image of the dried micelles (B).
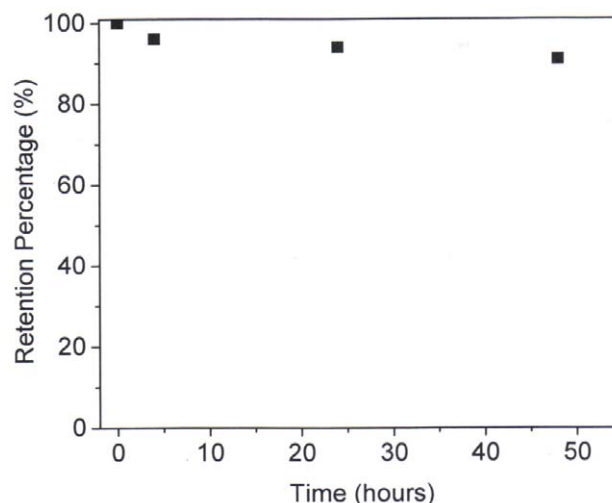doi:10.1371/journal.pone.0033390.g002

Figure 3. Retention percentage of PtTFPP from PCL-*b*-PEG micelles.
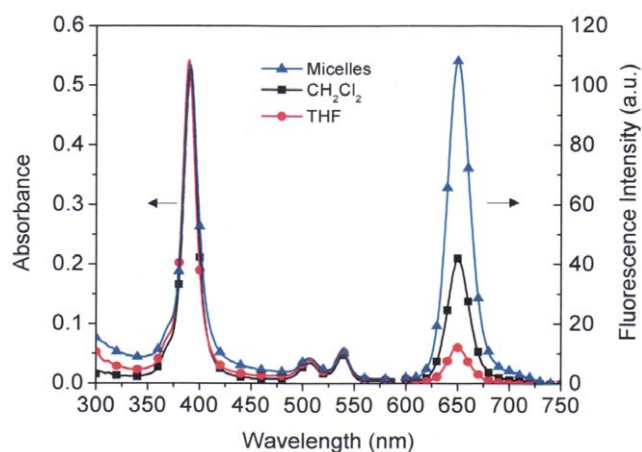doi:10.1371/journal.pone.0033390.g003

concentration of 2.5 µM. Absorbance of the micelle solution became broader than those in THF and CH_2Cl_2, indicating aggregations of PtTFPP molecules in the micelle cores. Interestingly, the emission of PtTFPP in the micelles was much stronger than those in THF and CH_2Cl_2, resulting in a higher quantum efficiency of PtTFPP in the micelles than those in THF and CH_2Cl_2. It was reported that quantum efficiency of PtTFPP in CH_2Cl_2 was 0.088 [41]. Quantum yield of PtTFPP in the micelles was calculated to be 0.110. A sugar modified PtTFPP, which is soluble in water, was reported to have a low quantum yield of 0.001 [45].

Quantum efficiency is affected by a few factors such as solvents, solvent polarity, fluorophore-fluorophore interactions, ordered and disordered aggregations [46]. Normally, the aggregated compounds show weaker emissions or exhibit lower fluorescence quantum yields than the monomeric fluorophore, due to a nonradiative decay. However, in the presence of micelles, the aggregates could be disrupted to their monomeric forms because

Figure 4. Photophysical properties of PtTFPP in micelles, THF and CH_2Cl_2 solutions.
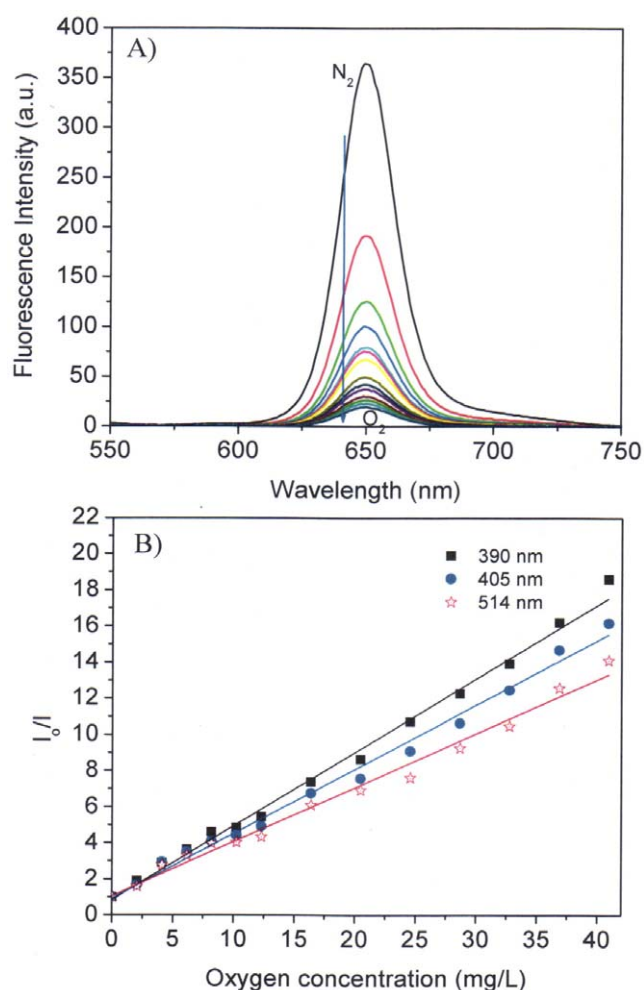doi:10.1371/journal.pone.0033390.g004

Figure 5. Typical oxygen sensing of the PtTFPP/PCL-*b*-PEG micelles excited at 390 nm (A). Stern-Volmer responses of the micelles excited at 390, 405, and 514 nm (B).
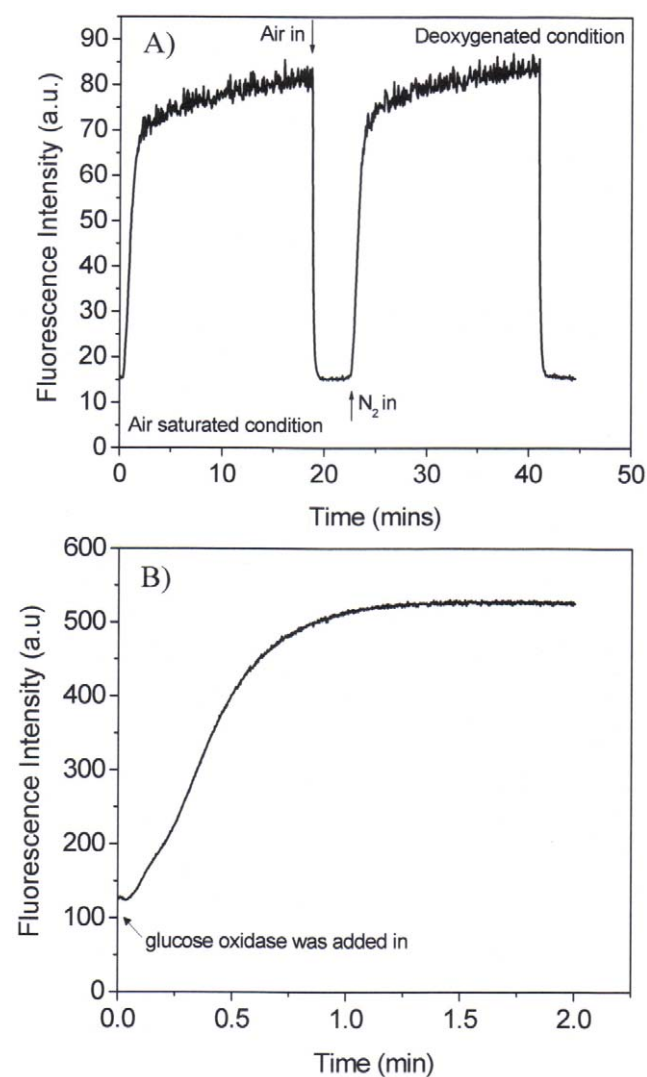doi:10.1371/journal.pone.0033390.g005

Figure 6. Response time studied through a saturation of air and nitrogen saturation to the micellar solutions (A) and through the consumption of the oxygen by the oxidation of glucose by glucose oxidase (B). Concentration of glucose was 0.25 M and the concentration of the glucose oxidase was 10 mg/mL.
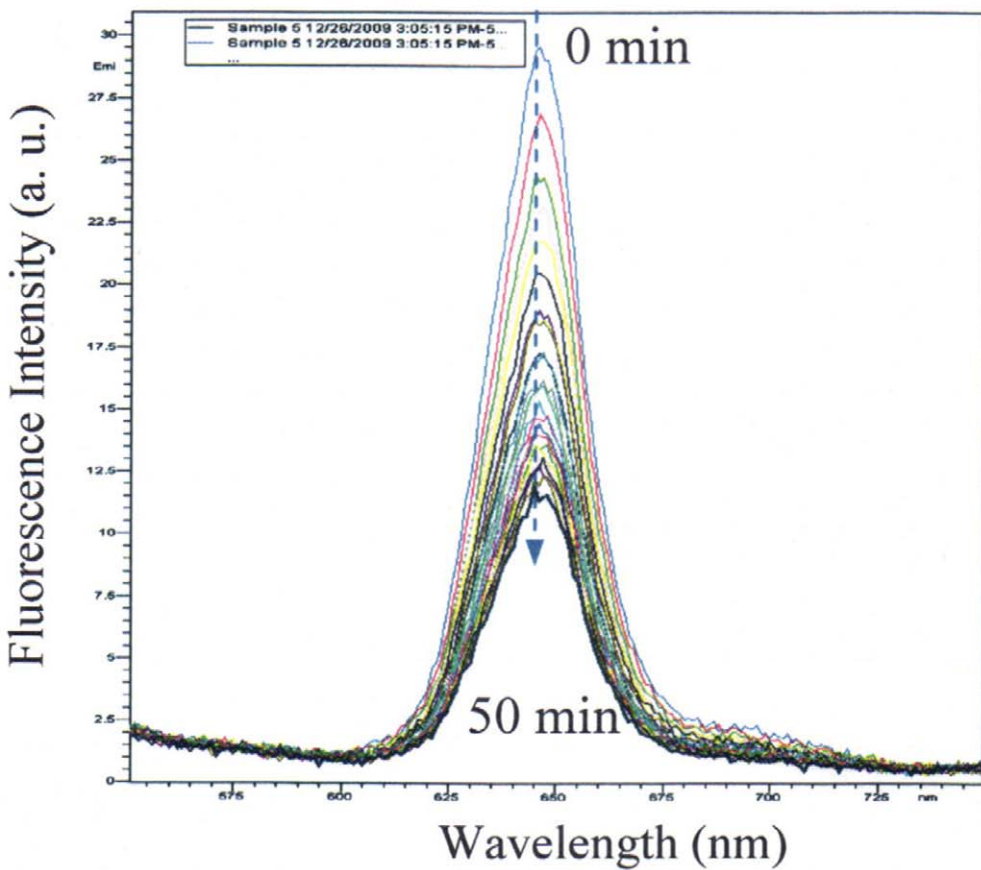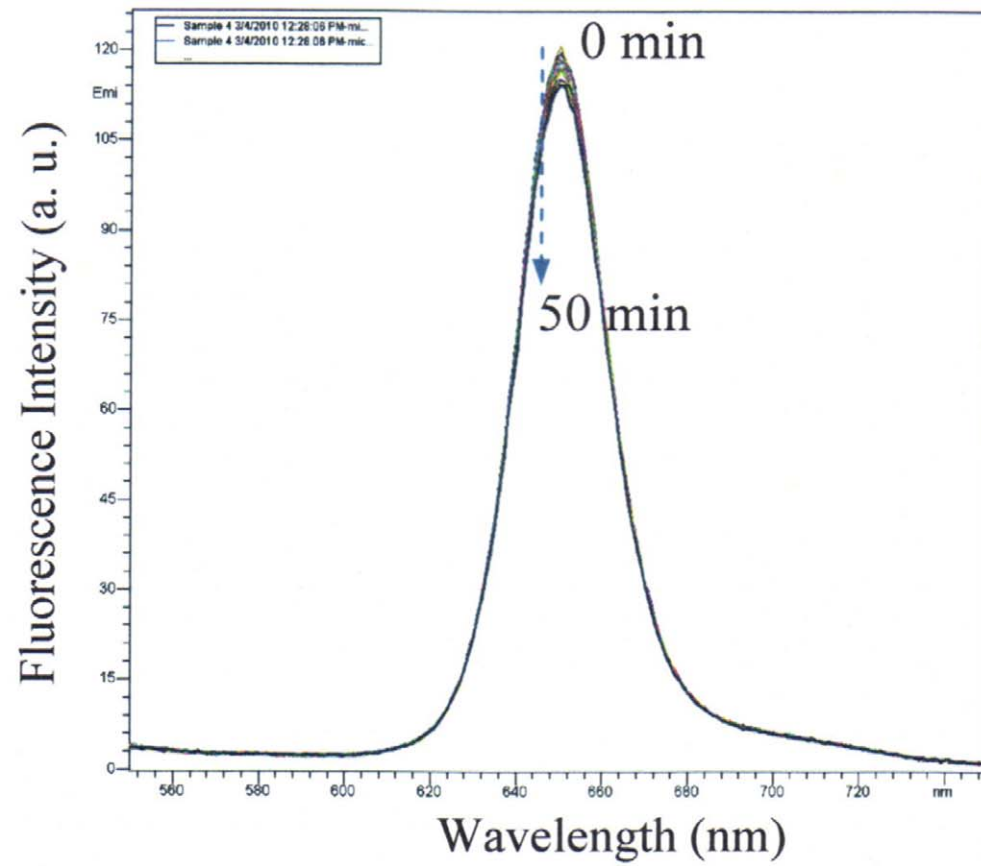doi:10.1371/journal.pone.0033390.g006

Figure 7. Photostability of PtTFPP in PCL-*b*-PEG micelles (A) and PtTFPP suspended in 5% THF-containing HEPES buffer (B).

of the distributions of fluorophores by the micellar cores formed from the hydrophobic polymers. This process will increase fluorescence quantum efficiency. When PtTFPP molecules were incorporated into the micelles, the PLC micellar cores forced the fluorophores to aggregate in the hydrophobic regions. However in the meantime, the PCL polymers could also have disrupted their aggregations. On the other hand, the polarity of PCL could also have affected the quantum yield. As a result of the combination effects of these, the quantum yield of PtTFPP in the micelles was higher than those in THF and CH_2Cl_2. When PtTFPP's concentrations were varied from 0.3125 μM to 2.5 μM, the quantum yields did not change much. All were within a range of 0.107 to 0.111.

Oxygen responses of PtTFPP in micelles

Dissolved oxygen concentrations were adjusted using a mixture gas of oxygen and nitrogen. The response to oxygen was shown in Figure 5A. Clearly, the emission of PtTFPP decreased with the increase of oxygen concentration. The intensity ratio (I_0/I) curves (Figure 5B) follows the Stern-Volmer equation as given in equation 2.

$$\frac{I_0}{I} = 1 + K_{SV}[O_2] \qquad (2)$$

where K_{SV} is the Stern-Volmer quenching constant. I_0 and I are the steady-state luminescence signals measured in the absence of oxygen and presence of different oxygen concentrations, respectively. $[O_2]$ is the dissolved oxygen concentration tuned by the nitrogen and oxygen mixed gas. Using the same optical set-up, excitation wavelength affected slightly on the Stern-Volmer quenching constants.

Response time

Using the air/nitrogen saturation method, it was found the response times, t_{95} (i.e., the time for 95% of the total change in fluorescence intensity to occur) and t_{99} (i.e., the time for 99% of the total change in fluorescence intensity to occur), were 52 and 68 s from the deoxygenated condition to the air saturated condition (Figure 6A), respectively. Recovery times from the air saturated solution to deoxygenated solution were slower with a $t_{95\text{-r}}$ of 380 s and $t_{99\text{-r}}$ of 760 s. These response times were quite close to those of PtTFPP physically doped in poly(2-hydroxyethyl methacrylate) (PHEMA) matrix and faster than those of PtTFPP physically doped in polystyrene (PS) matrix [25]. The t_{95} of PtTFPP in PHEMA and PS matrices from deoxygenated solutions to oxygenated solutions are 50 and 84 seconds, respectively [25]. This comparison demonstrated that these micelles may be reasonable materials for oxygen sensing.

Stationary state oxygen responsive time was studied using the deoxygenated approach with glucose oxidase through the oxidation of glucose and consumption of oxygen. (Figure 6B) The response time t_{95} is 50 seconds, in accordance with the time measured using the gas saturated approach with a t_{95} of 52 seconds. However, this response time is much slower than that of PtTFPP incorporated in the polystyrene-*block*-polyvinyl-pyrrolidone beads suspended in water, which has a t_{95} of about 4 seconds [37]. This indicates that polystyrene-*block*-polyvinylpyr-rolidone has a much faster gas permeable velocity than that of the PCL-*b*-PEG.

Photostability of the micelles

Photostability of PtTFPP in the micelles was compared with that of PtTFPP suspended in water under the same experimental conditions excited at 405 nm (0.2 mW/cm^2) for 50 minutes (Figure 7). Less than 5% fluorescence intensity decay was observed for the micelles after the 50 minutes of continuous light exposure. However, significant fluorescence decay (~60%) of PtTFPP dispersed in water was observed. The photostability study indicated that PtTFPP in the micelles could improve the probe's photostability. There are possibly two reasons for the high photostability of PtTFPP in water: (1) The hydrophobic micelle core alleviates the direct interaction of PtTFPP with water; (2) the aggregation of PtTFPP in micelles restricts the probe's molecules' movement. As a result of these two factors, the sensors are less reactive toward photo-oxidation and reduction to increase their photostability as compared to that of PtTFPP molecules directly interacting with water.

Conclusion

An amphiphilic block copolymer of PCL-*b*-PEG was applied to incorporate a popularly used oxygen sensor, PtTFPP, to enable the application of PtTFPP in aqueous solution. Micellar structures were observed from the PtTFPP/PCL-*b*-PEG assembled with an average diameter of 140 nm, confirmed using DLS and AFM. Interestingly, it was found that PtTFPP exhibited greater photostability in the micelles than when it was suspended in water. PtTFPP has good oxygen sensitivity and response time in the micelles, suggesting that it has great potential in its applications for oxygen sensing in biological systems. Further uses of these sensors for intracellular oxygen sensing are in progress.

References

1. Amao Y (2003) Probes and polymers for optical sensing of oxygen. Microchim Acta 143: 1–12.
2. Nagl S, Wolfbeis OS (2007) Optical multiple chemical sensing: status and current challenges. Analyst 132: 507–511.
3. Evans NTS, Naylor PFD (1967) The oxygen tension gradient across human epidermis. Resp Physiol 3: 38–42.
4. Huch R, Lubbers DW, Huch A (1974) Reliability of transcutaneous monitoring of arterial pO$_2$ in newborn infants. Arch Dis Child 49: 213–218.
5. Mitsubayashi K, Wakabayashi Y, Murotomi D, Yamada T, Kawase T, et al. (2003) Wearable and flexible oxygen sensor for transcutaneous oxygen monitoring. Sens Actuators B 95: 373–377.
6. Pang HL, Kwok NY, Chow LMC, Yeung CH, Wong KY, et al. (2007) ORMOSIL oxygen sensors on polystyrene microplate for dissolved oxygen measurement. Sens Actuators B 123: 120–126.
7. Lidstrom ME, Meldrum DR (2003) Life-on-a-chip. Nat Rev Microbiol 1: 158–164.
8. Molter TW, McQuaide SC, Suchorolski MT, Strovas TJ, Burgess LW, et al. (2009) A microwell array device capable of measuring single-cell oxygen consumption rates. Sens Actuators B 135: 678–686.
9. Zhang G, Palmer GM, Dewhirst MW, Fraser CL (2009) A dual-emissive-materials design concept enables tumour hypoxia imaging. Nature Materials 8: 747–751.

10. Thomas PC, Halter M, Tona A, Raghavan SR, Plant AL, et al. (2009) A noninvasive thin film sensor for monitoring oxygen tension during *in vitro* cell culture. Anal Chem 81: 9239–9246.

11. Garcia-Fresnadillo D, Marazuela MD, Moreno-Bondi MC, Orellana G (1999) Luminescent Nafion membranes dyed with ruthenium(II) complexes as sensing materials for dissolved oxygen. Langmuir 15: 6451–6459.

12. Amao Y, Okura I (2003) Optical oxygen sensing materials: chemisorption film of ruthenium(II) polypyridyl complexes attached to anionic polymer. Sens Actuators B 88: 162–167.

13. Xu H, Aylott JW, Kopelman R, Miller TJ, Philbert MA (2001) A real-time ratiometric method for the determination of molecular oxygen inside living cells using sol-gel-based spherical optical nanosensors with applications to rat C6 Glioma. Anal Chem 73: 4124–4133.

14. McEvoy AK, McDonagh C, MacCraith BD (1997) Optimisation of sol-gel-derived silica films for optical oxygen sensing. J Sol-Gel Sci Technol 8: 1121–1125.

15. Roche P, Al-Jowder R, Narayanaswamy R, Young J, Scully P (2006) A novel luminescent lifetime-based optrode for the detection of gaseous and dissolved oxygen utilising a mixed ormosil matrix containing ruthenium (4,7-diphenyl-1,10-phenanthroline)$_3$Cl$_2$ (Ru.dpp). Anal Bioanal Chem 386: 1245–1257.

16. Borisov SM, Vasylevska AS, Krause C, Wolfbeis OS (2006) Composite luminescent material for dual sensing of oxygen and temperature. Adv Funct Mater 16: 1536–1542.

17. Kimura F, Khalil G, Zettsu N, Xia Y, Callis J, et al. (2006) Dual luminophore polystyrene microspheres for pressure-sensitive luminescent imaging. Meas Sci Technol 17: 1254–1260.

18. Köse ME, Carrol BF, Schanze KS (2005) Preparation and spectroscopic properties of multiluminophore luminescent oxygen and temperature sensor films. Langmuir 21: 9121–9129.

19. McDonagh C, Burke CS, MacCraith BD (2008) Optical chemical sensors. Chem Rev 108: 400–422.

20. Vander Donckt E, Camerman B, Herne R, Vandeloise R (1996) Fibre-optic oxygen sensor based on luminescence quenching of a Pt(II) complex embedded in polymer matrices. Sens Actuators B 32: 121–127.

21. DeRosa M, Mosher P, Yap G, Foscaneanu K, Crutchley R, et al. (2003) Synthesis, characterization, and evaluation of [Ir(ppy)$_2$(vpy)Cl] as a polymer-bound oxygen sensor. Inorg Chem 42: 4864–4872.

22. Borisov SM, Klimant I (2007) Ultrabright oxygen optodes based on cyclometalated iridium(III) coumarin complexes. Anal Chem 79: 7501–7509.

23. Pauly S (1989) Permeability and diffusion data. Polymer Handbook, 3rd ed Brandrup J, Immergut EH, eds. John Wiley & Sons: New York, Chapter 6. pp 435–449.

24. Clark LC (1956) Monitor and control of blood and tissue oxygen tensions. Trans Am Soc Artif Intern Organs 2: 41–48.

25. Tian YQ, Shumway BR, Meldrum DR (2010) A new crosslinkable oxygen sensor covalently bonded into poly(2-hydroxyethyl methacrylate)-*co*-polyacrylamide thin film for dissolved oxygen sensing. Chem Mater 22: 2069–2078.

26. Tian YQ, Shumway BR, Gao W, Youngbull C, Holl MR, et al. (2010) Influence of matrices on oxygen sensing of three sensing films with chemically conjugated platinum porphyrin probes and preliminary application for monitoring of oxygen consumption of Escherichia coli (E. coli). Sens Actuators B 150: 579–587.

27. Tian YQ, Shumway BR, Youngbull AC, Li Y, Jen AKY, et al. (2010) Dually fluorescent sensing of pH and dissolved oxygen using a membrane made from polymerizable sensing monomers. Sens Actuators B 147: 714–722.

28. Ji J, Rosenzweig Z, Rosenzweig N, Jones I (2002) Novel fluorescent oxygen indicator for intracellular oxygen measurements. J Biomed Opt 7: 404–409.

29. Sud D, Zhong W, Beer D, Mycek MA (2005) Measurement of intracellular oxygen levels using fluorescence lifetime imaging microscopy (FLIM). Proc SPIE 5859: 585907-1–585907-10.

30. Koo YEL, Cao Y, Kopelman R, Koo SM, Brasuel M, et al. (2004) Real-time measurements of dissolved oxygen inside live cells by organically modified silicate fluorescent nanosensors. Anal Chem 76: 2498–2505.

31. McNamara KP, Rosenzweig Z (1998) Dye-encapsulating liposomes as fluorescence-based oxygen nanosensors. Anal Chem 70: 4853–4859.

32. O'Riordan TC, Fitzgerald K, Ponomarev GV, Mackrill J, Hynes J, et al. (2007) Sensing intracellular oxygen using near-infrared phosphorescent probes and live-cell fluorescence imaging. Am J Physiol Regul Inter Comp Physiol 292: R1613–R1620.

33. Saito T, Asakura N, Kamachi T, Okura I (2007) Oxygen concentration imaging in a single living cell using phosphorescence lifetime of Pt-porphyrin. J Porphyrins Phthalocyanines 11: 160–164.

34. O'Donocan C, Hynes J, Yashunski D, Papkovsky B (2005) Phosphorescent oxygen-sensitive materials for biological applications. J Mater Chem 15: 2946–2951.

35. Lee SK, Okura I (1997) Photostable optical oxygen sensing material: platinum tetrakis(pentafluorophenyl)porphyrin immobilized in polystyrene. Anal Commun 34: 185–188.

36. Han BH, Manners I, Winnik MA (2005) Phosphorescence quenching of dyes adsorbed to silica thin-layer chromatography plates. Anal Chem 77: 8075–8085.

37. Borisov SM, Mayr T, Klimant I (2008) Poly(styrene-*block*-vinylpyrrolidone) beads as a versatile material for simple fabrication of optical nanosensors. Anal Chem 80: 573–582.

38. Tian YQ, Wu WC, Chen CY, Jang SH, Zhang M, et al. (2010) Utilization of micelles formed from poly(ethylene glycol)-block-poly(ε-caprolactone) copolymers as nanocarriers to enable hydrophobic red two-photon absorbing (2PA) emitters for cells imaging. J Biomed Mater Resear A 93A: 1068–1079.

39. Tian YQ, Chen CY, Cheng YJ, Young AC, Tucker NM, et al. (2007) Hydrophobic chromophores in aqueous micellar solution showing large two-photon absorption cross-sections. Adv Funct Mater 17: 1691–1697.

40. Chen CY, Tian YQ, Cheng YJ, Young AC, Ka JW, et al. (2007) Two-photon absorbing block copolymer as a nanocarrier for porphyrin - energy transfer and singlet oxygen generation in micellar aqueous solution. J Am Chem Soc 129: 7220–7221.

41. Lai SW, Hou YJ, Che CM, Pang HL, Wong KY, et al. (2004) Electronic spectroscopy, photophysical properties, and emission quenching studies of an oxidatively robust perfluorinated platinum porphyrin. Inorg Chem 43: 3724–3728.

42. Joshi HS, Jamshidi R, Tor Y (1999) Conjugated 1,10-phenanthrolines as tunable fluorophores. Angew Chem Int Ed 38: 2721–2725.

43. Song HT, Choi JS, Huh YM, Kim S, Jun YW, et al. (2005) Surface modulation of magnetic nanocrystals in the development of highly efficient magnetic resonance probes for intracellular labeling. J Am Chem Soc 127: 9992–9993.

44. Lee J, Kim J, Park E, Jo S, Song R (2008) PEG-ylated cationic CdSe/ZnS QDs as an efficient intracellular labeling agent. Phys Chem Chem Phys 10: 1739–1742.

45. Hirohara S, Obata M, Alitomo K, Sharyo K, Ando T, et al. (2009) Synthesis and photocytotoxicity of S-glucosylated 5,10,15,20-tetrakis(tetrafluorophenyl)-porphyrin metal complexes as efficient ^{1}O$_2$-generating glycoconjugates. Bioconjugate Chem 20: 944–952.

46. Valeur B in Molecular Fluorescence: Principle and Applications, Chapter 7, Wiley-VCH, Weinheim, Germany 2002.